Pressure loss tests on a second model of a turbine volute

Bassett, R. W.; Murphy, C. L.

Publisher’s version / Version de l'éditeur:
https://doi.org/10.4224/40003764
Mechanical Engineering Test Report (National Research Council Canada. Division of Mechanical Engineering. Engine Laboratory); no. MET-365, 1962-08

NATIONAL RESEARCH COUNCIL OF CANADA

TEST REPORT

MET - 365

PRESSURE LOSS TESTS ON A SECOND MODEL OF A TURBINE VOLUTE

BY

R. W. BASSETT AND C. L. MURPHY

DIVISION OF MECHANICAL ENGINEERING

OTTAWA

AUGUST 1962

NATIONAL RESEARCH LABORATORIES

Ottawa, Canada

TEST REPORT

Division of Mechanical Engineering

Engine Laboratory

Pages - Preface	- 2		Test Report: MET-365
Text	- 5		Date: August 1962
App.	- 4		Lab. Order: 13387A
Figures	- 8		File: M2-17-13. T-6

For: Internal

Subject: PRESSURE LOSS TESTS ON A SECOND MODEL OF A TURBINE VOLUTE

Submitted by: M. S. Kuhring, Section Head

Authors: R. W. Bassett, C. L. Murphy

Approved by: D. C. MacPhail, Director

SUMMARY

This report presents the results of continued tests made on a second low-pressure model of a tip turbine volute duct having an axial discharge; this volute is different from the previous model in passage size and re-entry arrangement.

The over-all pressure loss, including the discharge nozzles, was measured and found to be 22 percent of the total gauge pressure in the supply duct. The tests indicated that 8.9 percent was lost in the volute duct, representing 26.7 percent of the dynamic head.

The static pressure along the inner and outer duct walls suggested that a free vortex velocity distribution existed in the duct and that the loss of static pressure was similar to that occurring along the walls of a straight pipe.

TABLE OF CONTENTS

LIST OF ILLUSTRATIONS

PRESSURE LOSS TESTS ON A SECOND MODEL OF A TURBINE VOLUTE

1.0 INTRODUCTION

Previous work on a model of the tip turbine volute duct and nozzle assembly had shown that about one-third of the loss of total pressure occurred in the duct, the remaining two-thirds being attributed to the nozzles. It was also found that the arrangement of the ducting at the "re-entry" point caused considerable disturbance to the flow entering the nozzles in this region.

In view of these findings a second model was constructed having a smaller duct area and incorporating a new "re-entry" arrangement.

The loss of total pressure has been measured with and without nozzle blades and comparisons have been made with the lower speed duct results reported in Reference 1, particularly in the re-entry region. Static pressures have been measured along the inner and outer walls of the duct and a comparison has been made with calculated values assuming a free vortex distribution.

2.0 TEST RIG AND INSTRUMENTATION

The test rig and instrumentation were similar to that described in Reference 1 with the following changes.

The square sectioned volute duct had an inlet area of 118 square inches instead of the 156 square inches previously used. The re-entry region provided for a maximum of 50 degrees overlap through which the two streams could be held parallel. Three sheet metal re-entry ducts were made permitting mixing at 0, 15, or 25 degrees beyond the tangent point. A plan view of the duct is shown in Figure 1.

The instrumentation was unchanged from that described in Reference 1. However, 0.030-inch diameter static taps were provided at mid-height along the inner and outer duct walls at 40-degree intervals.

3.0 TEST CONDITIONS

In order to achieve a nozzle outlet Reynolds number of 1.81×10^6 (based on nozzle span), a mean supply total pressure of 20.5 inches of water (gauge) was required for bladed tests. The resulting dynamic pressure in the duct was 6.82 inches of water and the Reynolds number based on the wall dimension varied from 9.61×10^5 at inlet to about 2.5×10^5 near the re-entry.

Bladeless tests were run at the same duct Reynolds number for which a mean supply total pressure of 12.2 inches of water was required.

4.0 BLADELESS VOLUTE

4.1 Outlet Conditions

Using the "Arrow Head" probe described and illustrated in Reference 1 traverses for total pressure and discharge angle were made at the nozzle exit plane. Readings were taken at 10-degree intervals around the discharge periphery at radial positions corresponding to 20, 50 and 80 percent span, related to the inner nozzle wall; the results are shown in Figures 2 and 3. In Figure 2 the outlet total pressure as a percentage of the mean supply total pressure is compared with that of the larger, lower speed, duct previously tested. The sudden change in outlet total pressure near the inner nozzle wall appears at a slightly different circumferential position, in fact about 20 degrees later. Again the decrease in total pressure is associated with an increase in discharge angle, signifying a change in the duct velocity profile.

The recorded values of total pressure were used to provide a mass weighted mean value and resulted in a measured loss of 1.87 inches of water, representing 26.7 percent of the duct dynamic head. The increase in loss above that of the larger duct is discussed in Section 5.0.

4.2 Re-Entry Studies

The traverses described in Section 4.1 were made with each of the three re-entry ducts. The results of these, shown in Figure 4, clearly indicate that the position at which the duct is ended after the tangent point has very little effect on conditions at the nozzle outlet.

A comparison with the larger duct results in this region (Fig. 2) does not show any of the expected improvement. The losses are still comparatively high in this area and have only been rearranged by the changes in duct geometry.

5.0 BLADED VOLUTE

5.1 Pressure Losses

Although nozzles specifically designed for this duct were not available, a set was fitted which had previously been tested on the larger duct. The over-all pressure loss was measured in the manner described in Reference 1 and found to be 4.5 inches of water or 22 percent of the supply total gauge pressure. Based on the assumption that the bladeless annular nozzle does not contribute significantly to the losses, the following table shows the division of loss between duct and nozzles, and compares the results with those of the larger duct.

Volute Inlet Area	156 in.^{2}		118 in.^{2}	
	In. H_20	% P_t Supply	In. H_20	% P_t Supply
Duct Dynamic Pressure	4.75		6.82	
Duct Loss	1.025	4.95	1.82	8.9
Nozzle Loss	2.125	10.25	2.68	13.1
Total Loss	3.15	15.2	4.50	22.0

The increase in nozzle loss from 10.25 percent to 13.1 percent was expected and resulted from the increased incidence placed on the blades by the higher tangential velocity in the duct.

The increase in duct loss from 4.95 to 8.9 percent of the supply pressure is caused by the higher dynamic head in the duct, the greater length to hydraulic diameter and possibly the re-arrangement of the re-entry region; the Reynolds number and the duct radius ratio do not differ significantly.

The effect of the higher duct velocity is obviously the major cause of the increased loss, since the loss increases only from 21.4 to 26.7 percent on the basis of dynamic pressure. The increased length to diameter ratio would account for most of this difference, but the effect of the re-entry change is difficult to evaluate.

5.2 Comparison of Nozzle Types

Cascade tests conducted independently on "flat-plate" nozzles had shown that a nozzle passage having a rectangular section, normal to the blades, had a lower loss coefficient than the trapezoidal sectioned nozzles originally designed. The two types are shown in Figure 5.

Three segments, each comprising six passages, of the rectangular section nozzles were tested in two positions at which detailed traverses had previously been made. The results of these tests are shown in the table below.

Position	$\Delta P_t/P_t$ Supply (Gauge) %	
	Trapezoidal	Rectangular
A	24.8	21.6
B	18.1	22.2

It can be seen that the cascade tests were not entirely confirmed. Other comparative tests were then made which showed clearly that the trapezoidal nozzle performance was much more dependent on the quality of a particular passage than on the circumferential position in which it was placed. In the tests reported in Reference 1 a considerable variation in the performance of individual nozzles was also found and was believed to have been caused by the roughness of the welding within the passages. The rectangular sectioned nozzles were fabricated by a method which avoided this exposed internal welding and resulted in a cleaner passage, giving more uniform results.

6.0 INTERNAL VOLUTE FLOW

The study of the flow in the volute duct was limited to the measurement of static pressure along the walls. These pressures, recorded at mid-height along the inner and outer walls, are shown in Figures 6 and 7. Pressure readings taken at positions above and below the mid-height position showed only minor differences.

In Figure 6 the radial pressure difference is plotted against circumferential position and is compared with the pressure difference calculated assuming a free vortex distribution (Appendix A). Very close agreement can be seen between 90 and 280 degrees. The deviation outside of this range is probably due to the inlet and re-entry disturbance. However, a free vortex distribution does appear to exist over most of the duct length.

The wall static pressures shown in Figure 7, in relation to the pressure level at the inlet measuring plane, can be seen to decrease along the outer wall and increase along the inner wall after the initial disturbances. The behaviour of these static pressures can be explained by the increasing radius ratio of the duct and is discussed further in Appendix A.

7.0 CONCLUSIONS

(1) The tangential re-entry did not reduce the high losses in this area but merely produced a slightly more uniform loss over a wider region.

(2) Decreasing the over-all unit diameter by reducing the duct area is expensive in terms of pressure loss. The change from 156 to 118 square inches, at inlet, increased the loss in the duct from 4.95 to 8.9 percent of the supply total gauge pressure, giving only about a 3-inch reduction in the over-all diameter.

(3) The increased loss with this smaller duct was almost entirely attributable to the higher duct velocities, the increase being only from 21.4 to 26.7 percent on the basis of dynamic pressure.

(4) The rectangular sectioned nozzle gave more consistent results because of the absence of welding within the passages, but did not clearly show a general improvement in performance.

(5) A free vortex distribution apparently exists in the duct over much of its length. The radius ratio is therefore a major factor controlling the pressure along the duct walls.

8.0 REFERENCES

1. Bassett, R. W. — Pressure Loss Tests on a Model of a Turbine Volute. NRC Test Report MET-328, August 1961.

2. Beij, K. H. — Pressure Losses for Fluid Flow in 90° Pipe Bends. U. S. National Bureau of Standards Journal, Vol. 21, July 1938, (Research Paper RP1110).

/LES

FIG. 1
MET-365

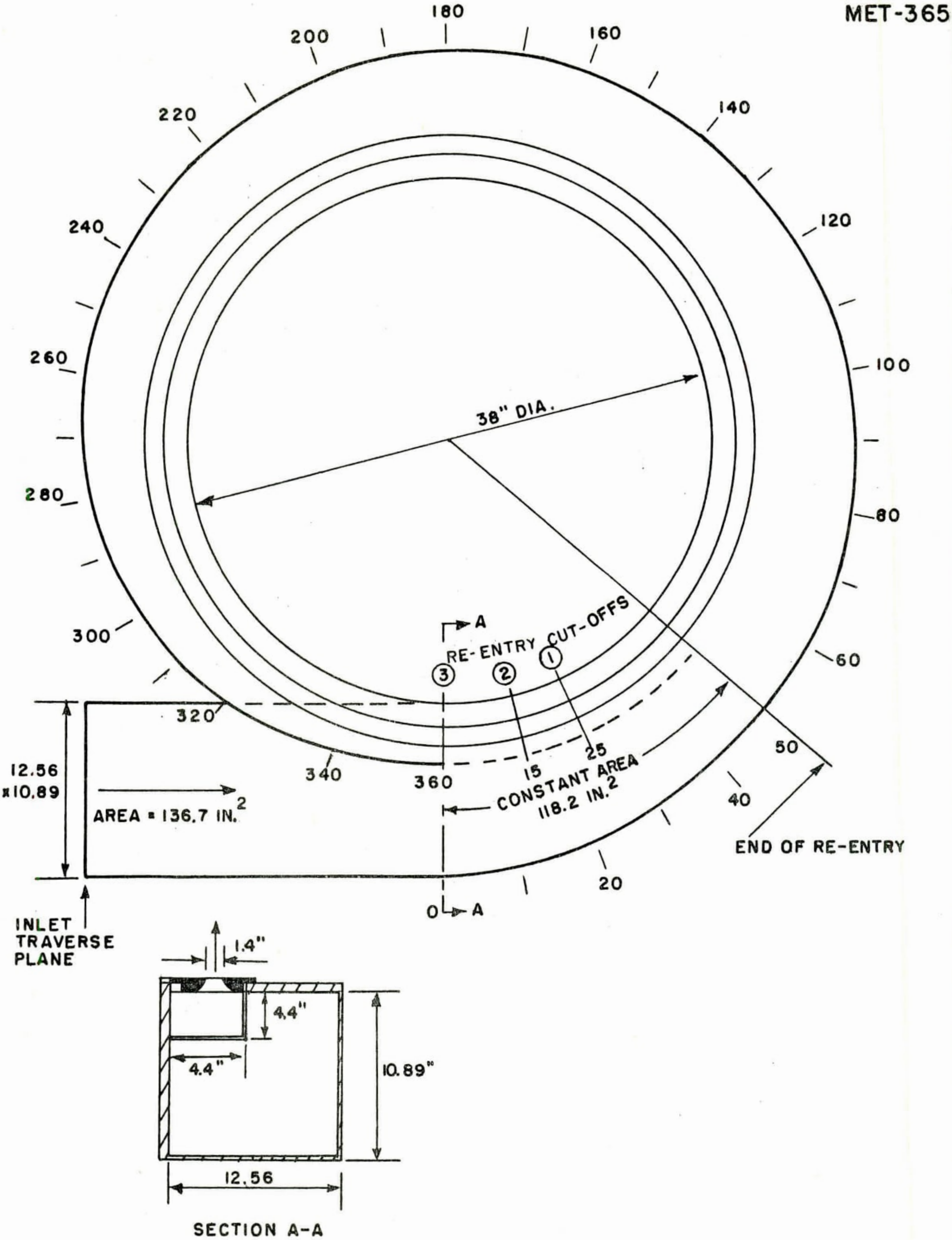

DIAGRAM OF VOLUTE

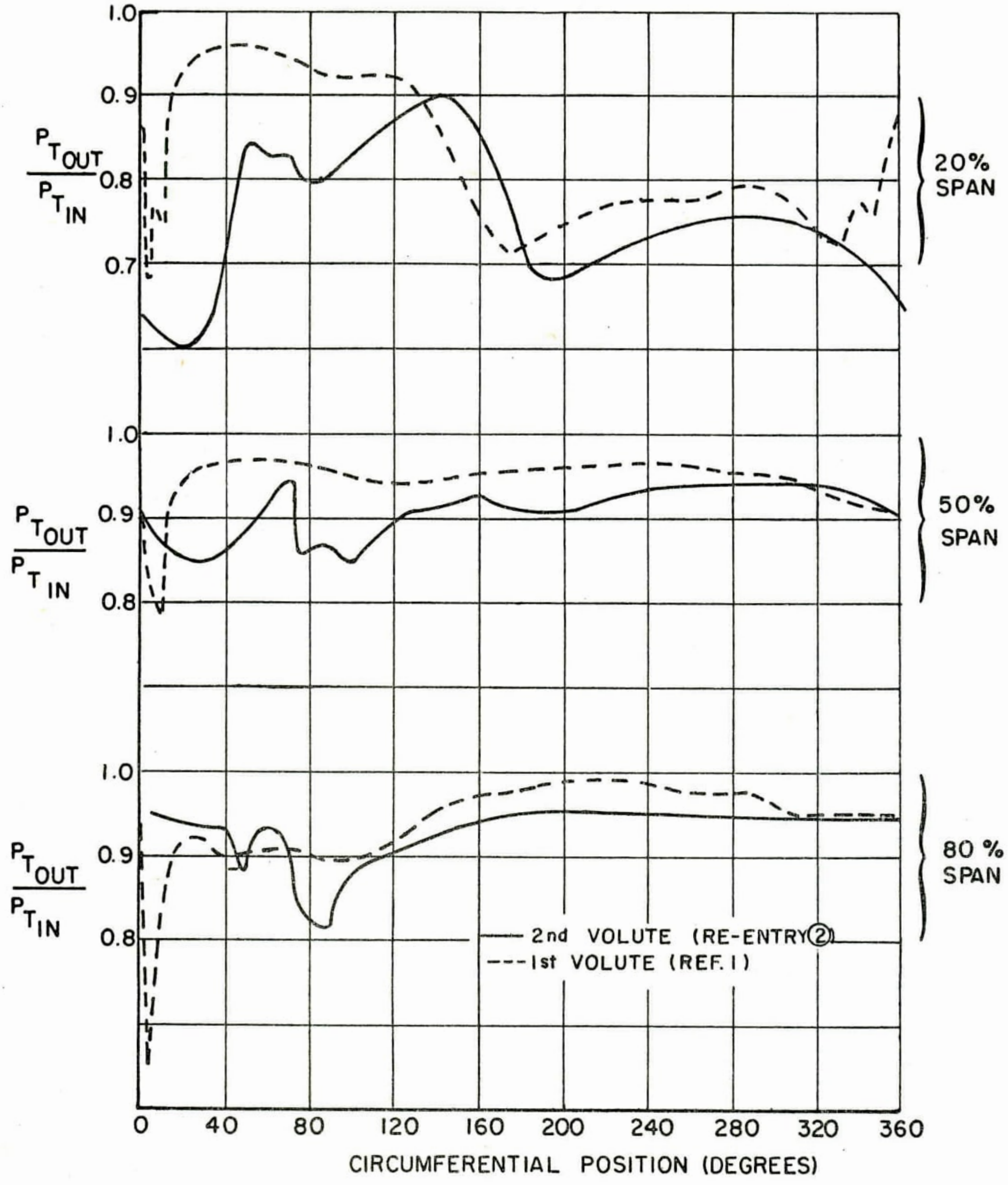

COMPARISON OF FIRST AND SECOND VOLUTES
TOTAL PRESSURE DISTRIBUTION – BLADELESS NOZZLE

FIG. 3
MET-365

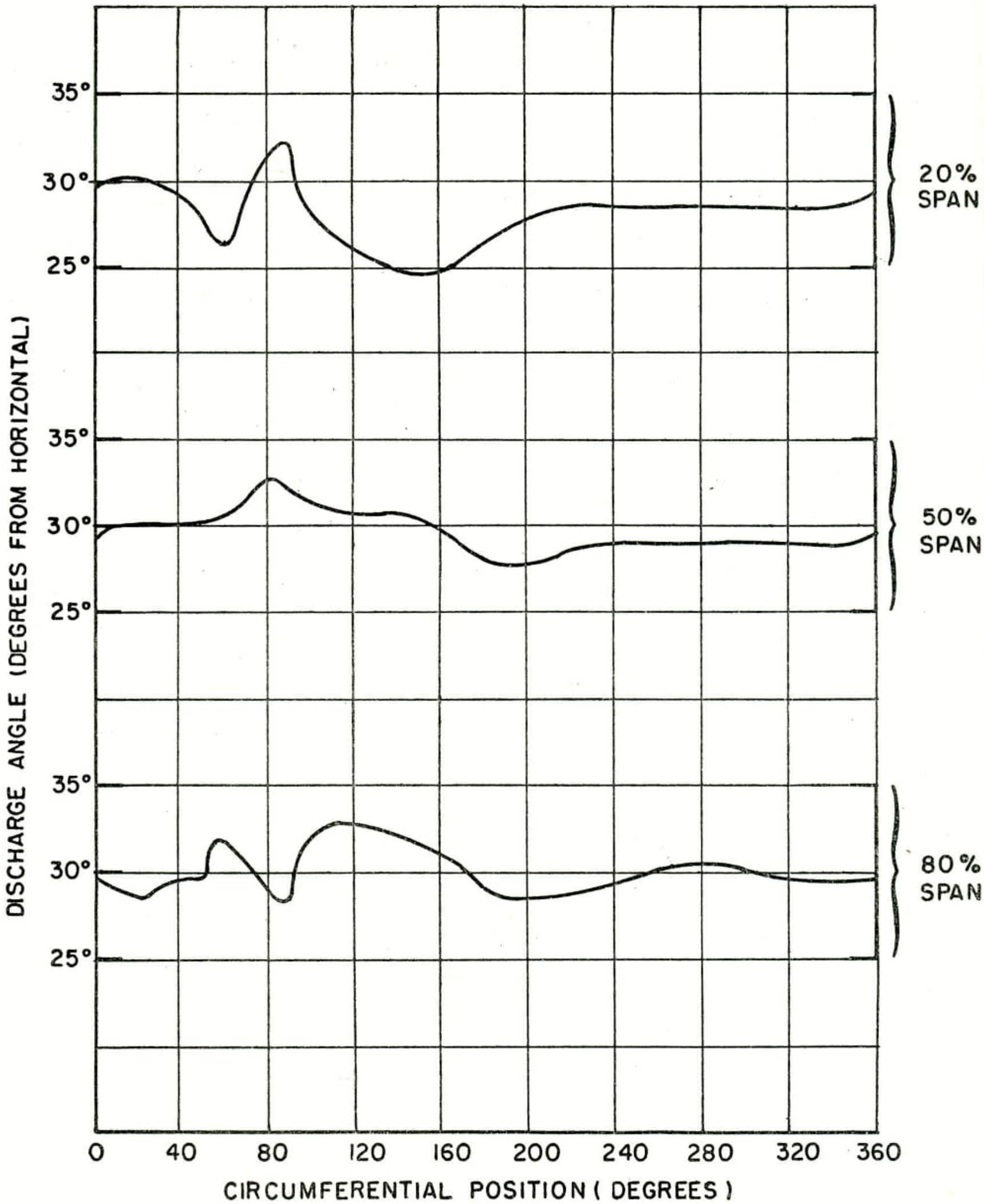

AIR DISCHARGE ANGLE — BLADELESS NOZZLE

FIG. 4
MET-365

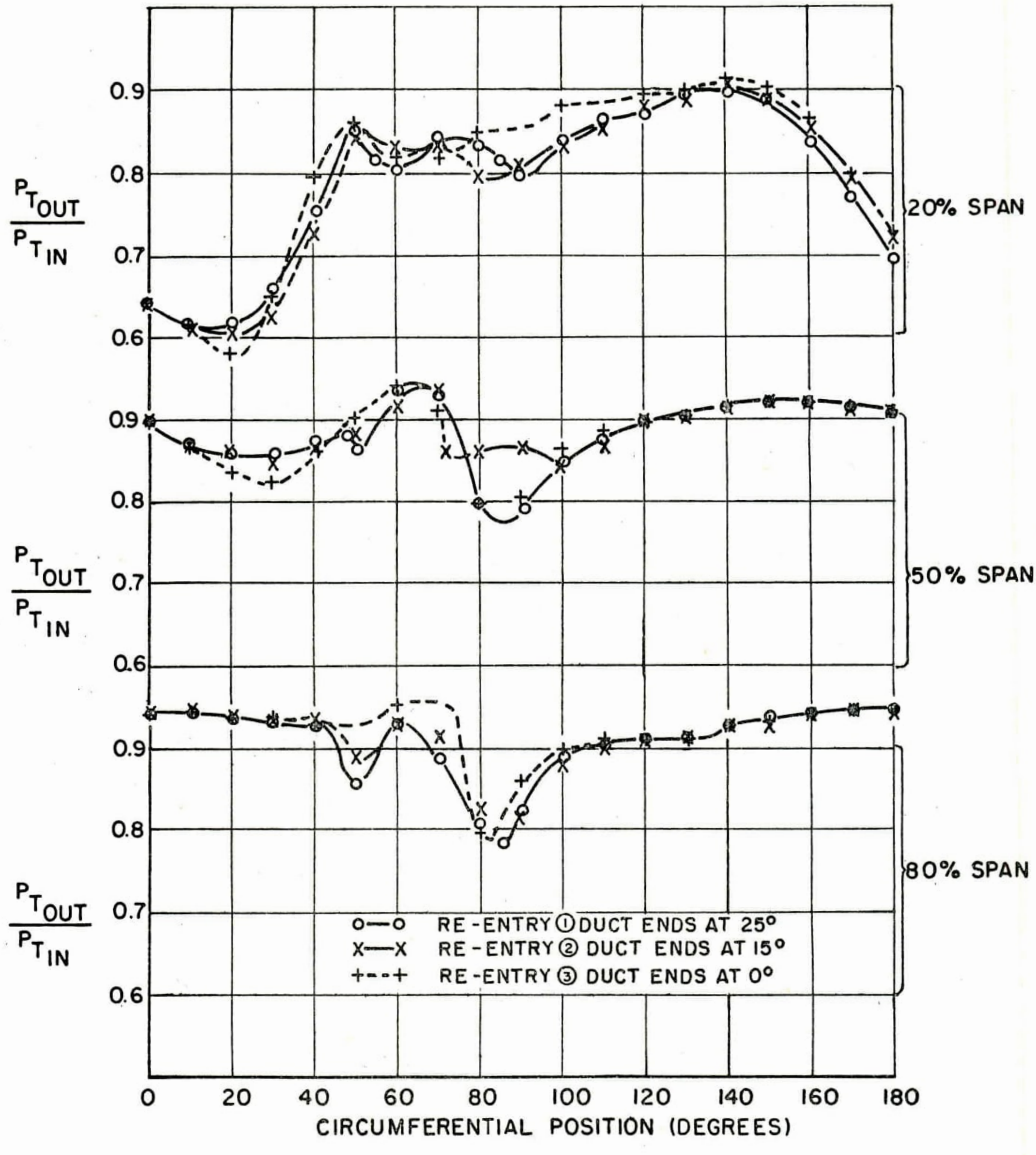

COMPARISON OF THREE RE-ENTRY PANELS
TOTAL PRESSURE DISTRIBUTION - BLADELESS NOZZLE

FIG. 5
MET-365

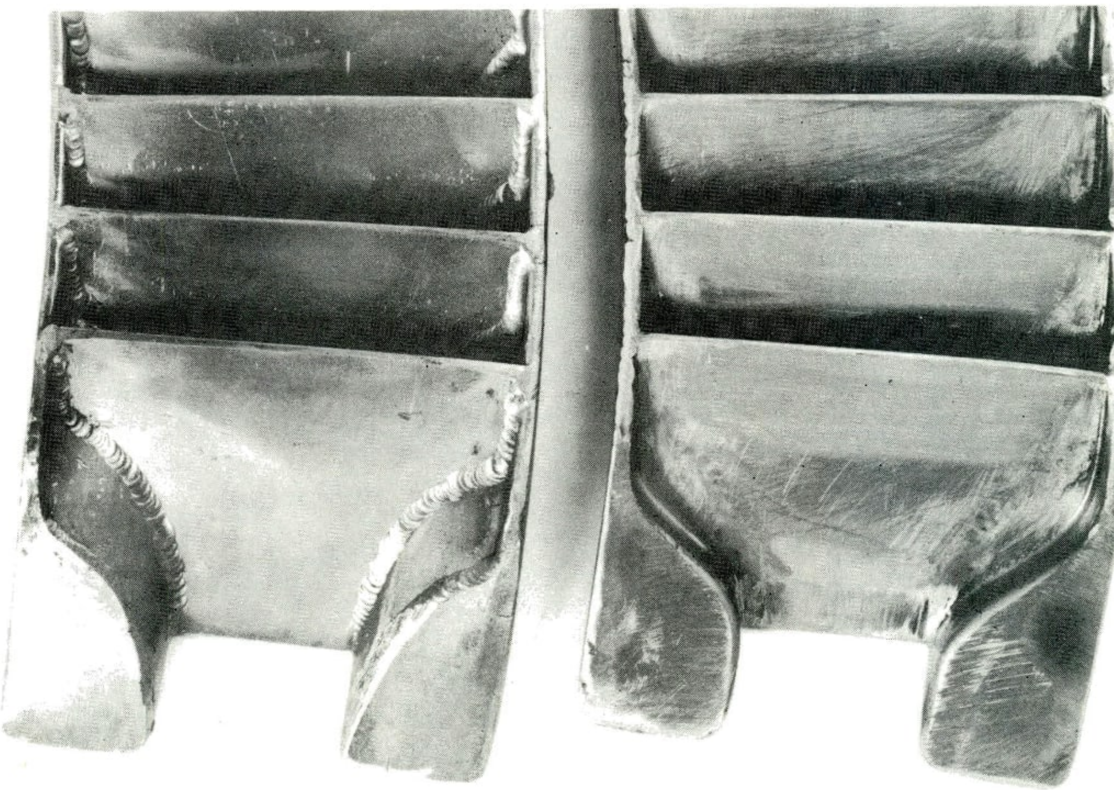

NOZZLE TYPES

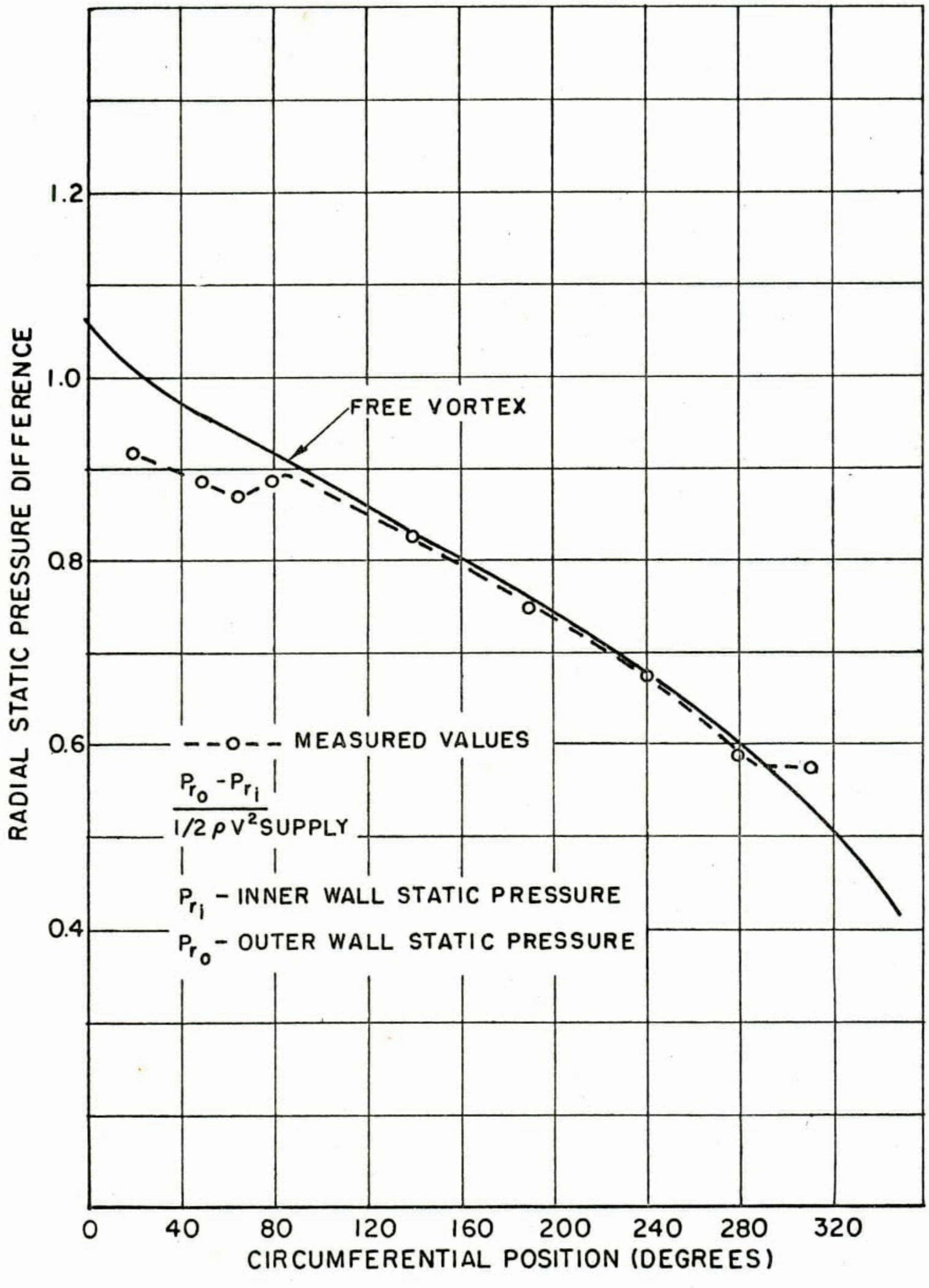

RADIAL STATIC PRESSURE DIFFERENCE AROUND VOLUTE DUCT

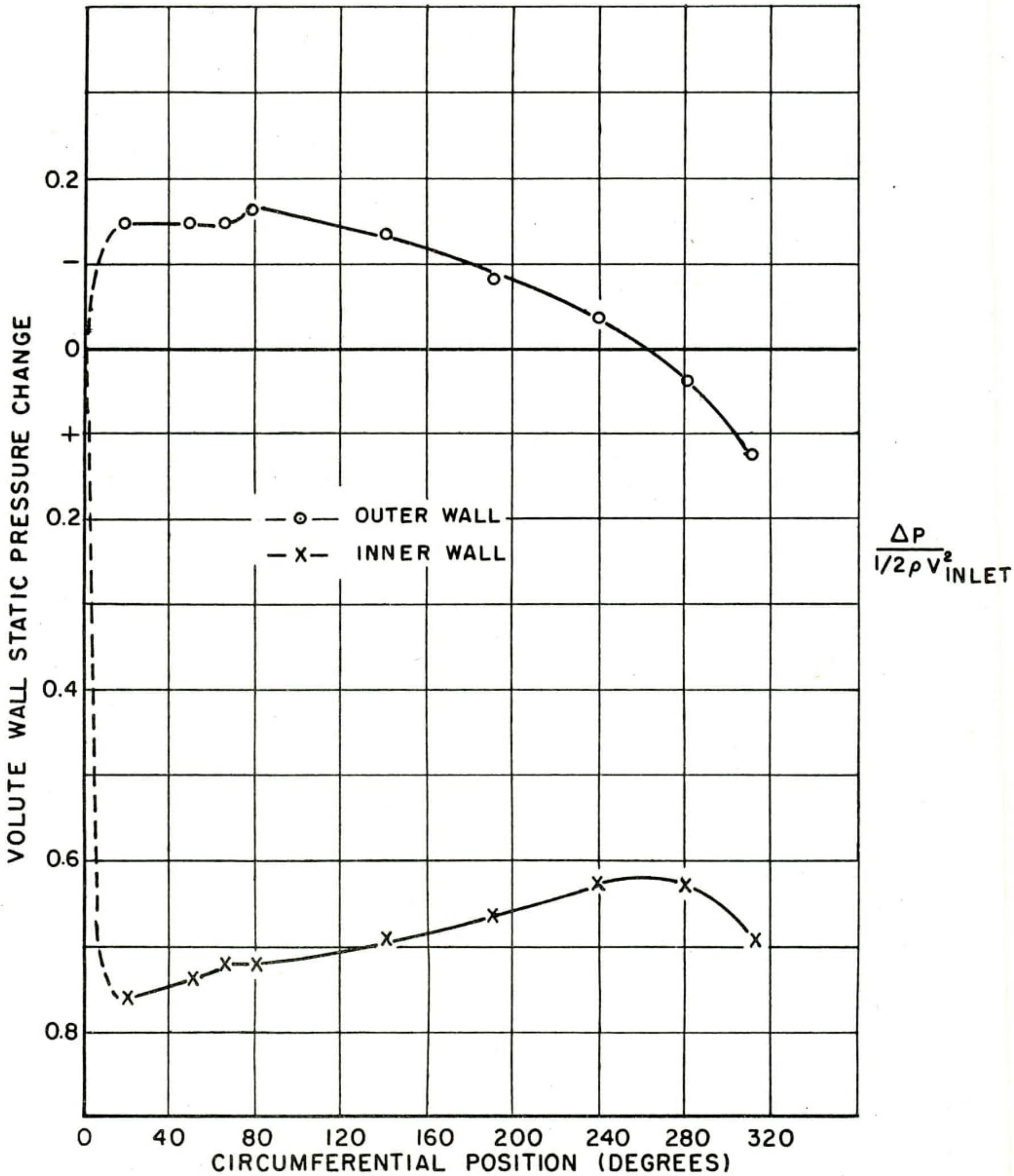

INNER AND OUTER WALL STATIC PRESSURE AROUND VOLUTE

APPENDIX A

ANALYSIS OF RADIAL PRESSURE FORCES IN A VOLUTE DUCT (INCOMPRESSIBLE FLOW)

A.1 DERIVATION OF BASIC PRESSURE DIFFERENCE EQUATION

When a fluid enters a bend a radial pressure force is produced as a result of centrifugal action.

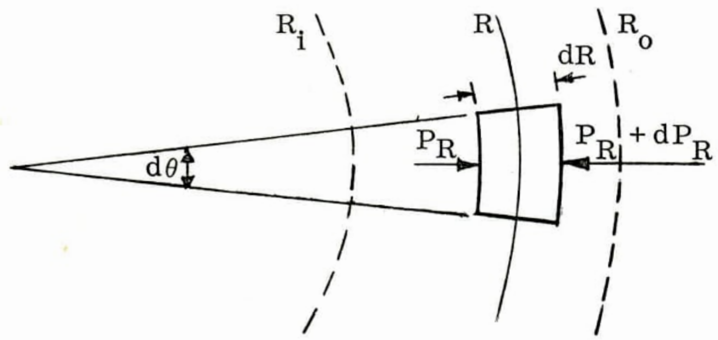

If the height of an element, of density ρ, is taken as b, then for radial equilibrium:

Outward Forces = Inward Forces

$$R\, d\theta\ b\, dR\, \rho\, \frac{V_t^2}{R} + R\, d\theta\ b\, P_R = R\, d\theta\ b\, (P_R + dP_R)$$

$$\rho\, \frac{V_t^2}{R}\, dR = dP_R \qquad \text{(a)}$$

If further a free vortex velocity distribution is assumed to exist across the duct, then

$$R\, V_t = \text{constant}$$

and equation (a) can be written

$$\frac{\rho\, (R\, V_t)^2\, dR}{R^3} = dP_R \qquad \text{(b)}$$

Integrating from R_o to R_i, the inner and outer radii of the duct

$$\int_{P_{R_i}}^{P_{R_o}} dP_R = \rho\,(R\,V_t)^2 \int_{R_i}^{R_o} \frac{dR}{R^3}$$

$$P_{R_o} - P_{R_i} = \frac{\rho\,(R\,V_t)^2}{2} \left[\frac{1}{R_i^2} - \frac{1}{R_o^2}\right] \qquad \text{(c)}$$

A. 2 RESTATEMENT OF PRESSURE DIFFERENCE EQUATION IN TERMS OF SUPPLY VELOCITY

Assuming the duct area is such as to produce an average velocity equal to that in the supply duct, V_s, then the equation of continuity gives:

$$\rho\, b\,(R_o - R_i)\,V_s = \rho\, b\,(R_o - R_i)\; \frac{\int_{R_i}^{R_o} V_t\, dR}{(R_o - R_i)}$$

$$(R_o - R_i)\,V_s = \int_{R_i}^{R_o} \frac{(V_t R)\,dR}{R}$$

$$= V_t\, R\, \log_e\left(\frac{R_o}{R_i}\right)$$

or

$$V_t\, R = \frac{V_s\,(R_o - R_i)}{\log_e\left(\frac{R_o}{R_i}\right)} \qquad \text{(d)}$$

Substitution in equation (c) for $(V_t\, R)^2$

$$P_{R_o} - P_{R_i} = \frac{\rho\, V_s^2}{2} \left(\frac{R_o - R_i}{\log_e\left(\frac{R_o}{R_i}\right)}\right)^2 \left[\frac{1}{R_i^2} - \frac{1}{R_o^2}\right]$$

or

$$\frac{P_{R_o} - P_{R_i}}{\frac{\rho V_s^2}{2}} = \left[\frac{R_o - R_i}{\log_e \frac{R_o}{R_i}}\right]^2 \left[\frac{1}{R_i^2} - \frac{1}{R_o^2}\right] \qquad (e)$$

In Figure 5, equation (e) is compared with the experimental values and gives very close agreement over much of the length of the duct. From this it is concluded that, away from the top and bottom walls, a free vortex distribution exists in the volute.

A. 3 DERIVATION OF WALL STATIC PRESSURES ASSUMING FRICTIONLESS FLOW

Assuming frictionless flow, the radius, $R_{m.v.}$, at which $V_t = V_s$ is also the radius at which the local static pressure equals the static pressure in the supply duct (P_s). By integration of equation (b) from R_o to $R_{m.v.}$ and R_i to $R_{m.v.}$ the static pressure change along the inner and outer walls is given by

$$\frac{P_s - P_{R_i}}{\frac{\rho V_s^2}{2}} = \left(\frac{R_o - R_i}{R_i \log_e \left(\frac{R_o}{R_i}\right)}\right)^2 - 1 \qquad (f)$$

and

$$\frac{P_s - P_{R_o}}{\frac{\rho V_s^2}{2}} = \left(\frac{R_o - R_i}{R_o \log_e \left(\frac{R_o}{R_i}\right)}\right)^2 - 1 \qquad (g)$$

A. 4 COMPARISON OF THEORETICAL AND EXPERIMENTAL WALL STATIC PRESSURES

These static pressure changes are shown in Figure A1 as a percentage of the average velocity head in the supply duct. Simple pipe friction loss, again based on the average velocity, has been added and the comparison with measured values is generally good. There is, however, a fairly constant difference between the predicted and measured pressure level, being about 8 percent of a velocity head. This suggests an excessive loss in the entry of the volute which would lower the pressure level rather than change the rate at which the pressure falls subsequently.

The radius ratio, which is the ratio of the mean radius of the bend to the radial width of the passage, varies in this volute from 2.25 to 4.8. In tests on circular-section 90-degree bends of radius ratios of about 3 to 4, Beij (Ref. 2) has found that the over-all static pressure drop is the same as in an equal length of straight pipe for fully developed flow. It appears reasonable, therefore, that the pressure should fall along the volute in a similar way and that it may be predicted by the simple method outlined, provided that the bend radius ratio is about 3 or 4.

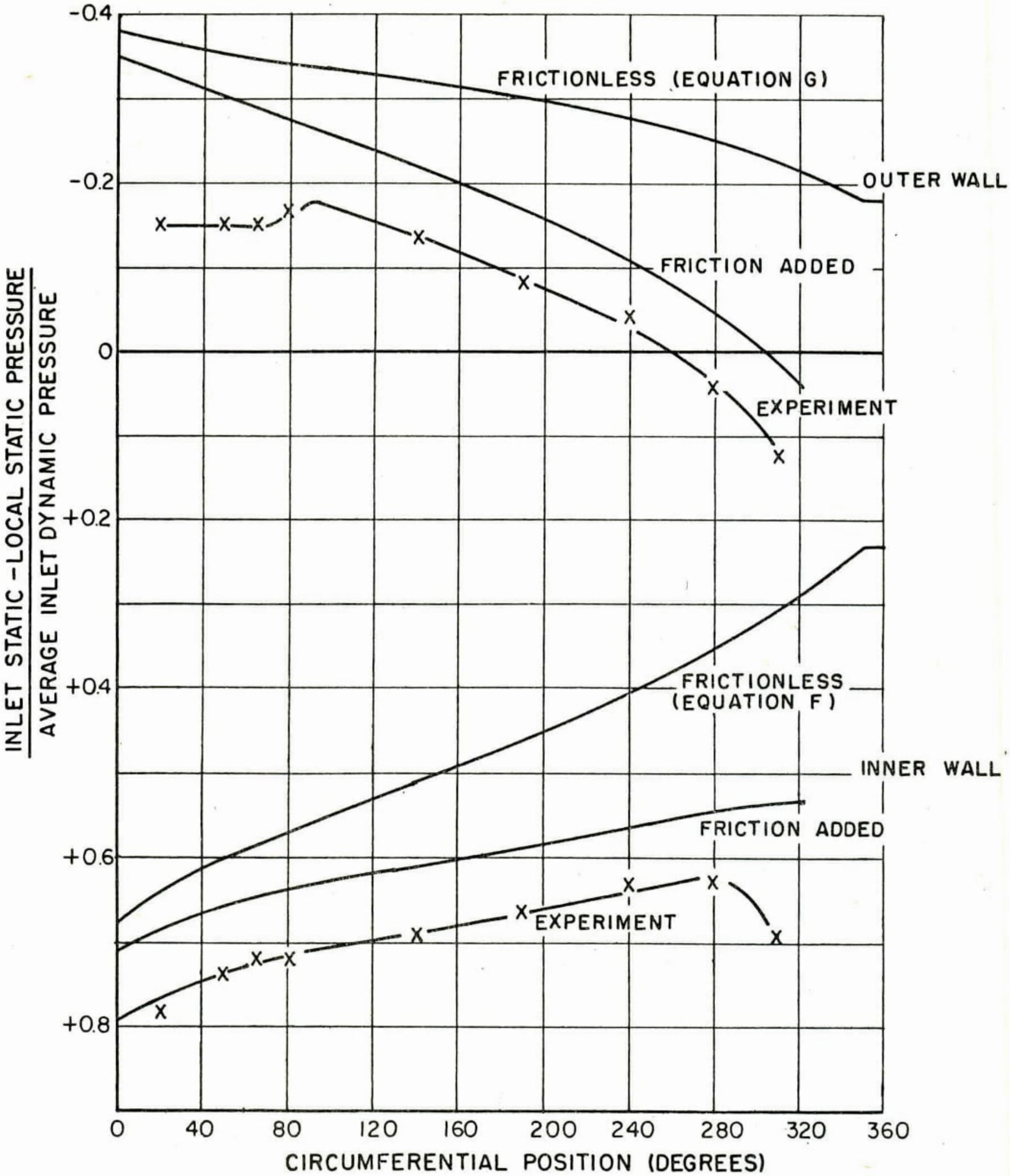

STATIC PRESSURES ALONG INNER AND OUTER VOLUTE DUCT WALLS